Semiconductor Physics, Quantum Electronics & Optoelectronics, 2026. V. 29, No 1. P. 051-056.

Semiconductor physics

Localized surface plasmon resonance and damping mechanisms in transition metals

F. Sila[1,2], B. Mbaluka[3], M. Riara[4] & N. Katumo[5]

[1]*South Eastern Kenya University, Department of Physical Sciences, P.O. Box 170–90200, Kitui, Kenya*
[2]*Umma University, Department of Physics, P.O Box 713–01100, Kajiado, Kenya*
[3]*Bomet University, Bomet, P.O. Box 701–20400, Bomet, Kenya*
[4]*Tharaka University, P.O. Box 193–60215, Marimanti, Kenya*
[5]*Fosep Technologies Ltd, P.O Box 17015–00100, Nairobi, Kenya*
[*]*Corresponding author e-mail: faithsila4242@gmail.com*

Abstract. This work reports the calculated dependence of the localized surface plasmon resonance (LSPR) parameters and damping mechanism on nanoparticle size of unconventional transition metals, including zinc, silver, rhodium, rhenium, molybdenum, tantalum, titanium, and scandium, within the size range of 10 to 400 nm. The study applies Mie theory to determine the peak energies, amplitude, and full width at half maximum (FWHM) of LSPR as a function of size, shape, and material type. We have found that the parameters of LSPR depend on electron structure and damping mechanisms. LSPR amplitude decreased systematically for individual nanoparticles (NPs) for sizes 10…200 nm, after which, a similar trend was exhibited due to radiative damping. Au, Sc and Ag are the only metal NPs that exhibited a significant FWHM of LSPR at sizes approximately below 40 nm. For all investigated transition metal NPs, smaller NPs exhibited higher absorption and lower scattering, while larger NPs showed narrower FWHM and red-shifted LSPR peaks due to retardation effects and multipolar plasmon excitations. The analysis highlights that some transition metal NPs exhibit optical characteristics similar to those of gold, silver, and copper, making them a good alternative for the mentioned ones at specific NP sizes.

Keywords: unconventional transition metals, scattering, absorption, localized surface plasmon resonance, damping, noble metals.

https://doi.org/10.15407/spqeo29.01.051
PACS 71.20.Be, 73.20.Mf, 73.22.-f

Manuscript received 21.10.25; revised version received 03.02.26; accepted for publication 18.03.26; published online 25.03.26.

1. Introduction

Noble metal nanoparticles, such as gold (Au) and silver (Ag), exhibit strong localized surface plasmon resonance (LSPRs) due to their electronic structures and low optical losses. LSPRs arise from the collective oscillation of conduction electrons in metallic nanoparticles (NPs) excited by incident electromagnetic radiation. These resonances give rise to strong optical absorption and scattering features whose spectral position and linewidth depend sensitively on NP size, geometry, material composition, and the surrounding dielectric environment [1, 2]. This enables applications in sensing, imaging, and photonics [3, 4].

Noble metals such as gold and silver are the most extensively studied plasmonic materials due to their strong and spectrally narrow LSPR responses in the visible region [5, 6]. Despite their widespread use, noble metals face several limitations, including high cost, limited natural abundance, and restricted spectral behaviour, particularly in the ultraviolet region where interband transitions lead to strong damping [7, 8]. These limitations have motivated increasing interest in alternative plasmonic materials, especially transition metals that are not traditionally classified as canonical plasmonic systems [9, 10].

In this work, the term "unconventional transition metals" (UTM) refers to metallic elements that are not conventionally used in plasmonic applications; however, they can support size-dependent collective electron oscillations under appropriate conditions [6, 11]. These include zinc (Zn), scandium (Sc), titanium (Ti), molybdenum (Mo), tantalum (Ta), rhenium (Re), and rhodium (Rh). Unlike Au and Ag, these metals often exhibited stronger intrinsic damping and interband transitions, but they also offer advantages such as broader spectral response, ultraviolet plasmonic activity, chemical robustness, and cost effectiveness [12, 13].

Table. Transition metals and the selection criteria for this study.

Group	Transitional elements	Serial number	Abundance	Synthesizability of NPs	Stability
3	scandium (Sc)	21	moderately	possible	stable
4	titanium (Ti)	22	abundant	possible	stable
5	tantalum (Ta)	73	low	possible	stable
6	molybdenum (Mo)	42	abundant	possible	stable
7	rhenium, Re	75	rare metal (costly)	possible	stable
9	rhodium, Rh	45	rare	possible	stable
11	silver (Ag)	28	relatively abundant	possible	stable
	gold(Au)	78	relatively abundant	possible	stable
12	zinc (Zn)	30	abundant	possible	exists as an oxide

Au and Ag are included in this study as reference benchmarks to contextualize the plasmonic behaviour of the unconventional metals [10, 14]. Recent advances in nanoplasmonics have demonstrated that several transition metals can exhibit tunable LSPR responses, particularly in the ultraviolet and broadband spectral regions, making them promising candidates for sensing, catalysis, and energy-related applications [15, 16]. However, systematic studies examining how the NP size dependence of the LSPR peak position and damping behavior across a wide range of unconventional transition metals remain limited.

This study addresses this gap by performing a comparative, size-dependent theoretical analysis of LSPR peak energies and linewidths for the range of unconventional transition metal NPs with diameters ranging from 10 to 400 nm, using full Mie theory.

2. Methods

The characteristics of the transition metals used in this study are listed in Table.

The optical dependences have been analyzed for NPs with sizes ranging from 10 to 400 nm with intervals of 10 up to 200 nm and thereafter 20 nm [17].

Complex refractive indices ($n + ikn + ik$) for each metal were obtained from experimentally validated sources *via* refractiveindex.info, with original references cited (*e.g.* [18] for Au). Data were digitized and incorporated into a custom MATLAB-based Mie solver ("MieApp") to calculate scattering, absorption, and extinction cross-sections for spherical NPs in vacuum. The NP diameters were varied from 10 to 400 nm, with a step of 10 nm (up to 200 nm) and 20 nm (beyond 200 nm).

The LSPR peak energy and the full width at half maximum (FWHM) were extracted from extinction spectra. The scattering to absorption ratio was calculated at the LSPR maximum. Results were validated using an online Mie calculator [10, 19, 20].

From the Mie scattering and absorption function, FWHM, plasmonic (peak energy), and scattering/absorption ratio at different NP sizes were obtained. The extracted data were used to determine the electronic properties of NPs of different sizes by calculating the light scattering intensity as a typical inverse problem [21]. This research adopted an inverse mathematical model, which is based on Mie scattering. It deduced the inversion formulas for particle size and calculated the relative coefficients by programming with built-in functions in MATLAB. Scattering and absorption curves were plotted using Origin software from the data obtained in "MieApp". Fig. 1 shows the steps taken to code in MATLAB software.

3. Results and discussions

3.1. Size-dependence of the LSPR peak position

As a first step, we used Au NPs as a reference system to validate the numerical implementation of the Mie theory and to establish a reliable base for interpreting the size-dependent plasmonic trends of uncommon plasmonic metals. The optical behavior of Au NPs, including the transition from absorption-dominated to scattering-dominated regimes and the red shift of the dipolar LSPR with increasing NP size, is extensively documented in the literature and is not claimed as a novel result in this

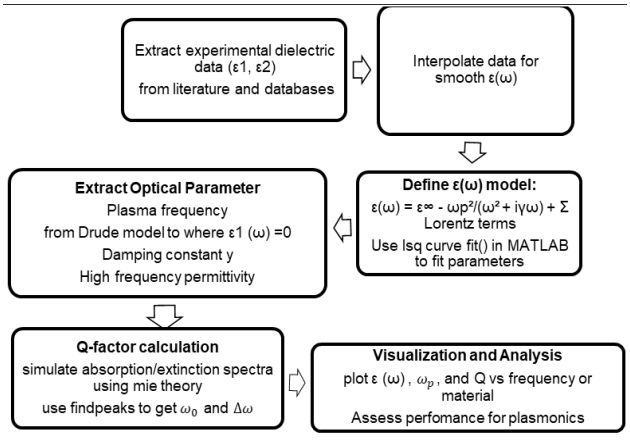

Fig. 1. MATLAB-based workflow for extracting dielectric functions from literature data, fitting the Drude–Lorentz model, and evaluating plasmonic performance parameters.

study. For small Au NPs, approximately 30 nm in diameter, absorption dominated the optical response due to strong dipolar LSPR excitation. As the NP size increases, scattering becomes increasingly significant, eventually surpassing absorption for diameters above approximately 80…100 nm due to enhanced radiative damping and retardation effects. The red shift of the LSPR peak with increasing size arises from phase retardation across the particle and the emergence of higher-order multipolar plasmon modes. The scattering-to-absorption ratio is discussed qualitatively, as the spectral maxima of scattering and absorption are not strictly aligned; consequently, the ratio depends on the relative spectral positions of these maxima and should not be interpreted as an intrinsic material constant.

Fig. 2 presents the dependence of the LSPR peak energy on NP size for the selected noble metals and UTMs. For all materials, the LSPR peak exhibited a systematic red shift with increasing NP size. At small sizes, below approximately 200 to 275 nm, the LSPR energy showed strong material dependence, reflecting differences in electron density, electronic band structure, and dielectric response among the metals. At larger sizes, the LSPR peak energies converged across different materials and became predominantly size-dependent rather than material-dependent. This convergence arises from dynamic depolarization and retardation effects, which reduce the influence of intrinsic electronic properties on the collective electron oscillation. Several unconventional transition metals, including Mo, Ti, Rh, and Re, exhibited high-energy LSPR peaks in the UV range for small NPs, highlighting their potential for UV and broadband plasmonic applications.

It's clearly observed that there is pronounced material dependence of the LSPR energies in the range of small NP sizes, approximately between 10 and 275 nm. In contrast, for large NPs, the LSPR energy is material-independent and depends only on the NP size.

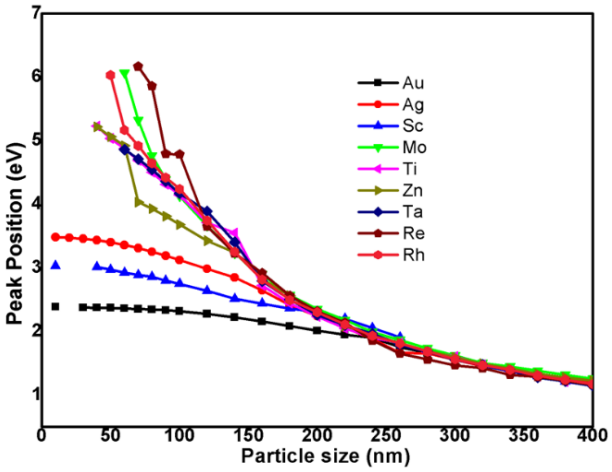

Fig. 2. The dependence of LSPR peak energy as a function of nanoparticle diameter for selected noble (Au, Ag) and transition metals (Sc, Mo, Ti, Zn, Ta, Re, and Rh).

The material-dependent behavior for the small NPs is related to the strong dependence of the LSPR energy on electron density and to a smaller extent on differences in the real parts of the dielectric response function for various transition metals. The material independence of the LSPR energy observed for large NPs is caused by the significant role of dynamic depolarization. As the NP size increases, the LSPR energy shifts to the red side, and finally, the period of the collective electron oscillations becomes of the same order of magnitude as the retardation time needed to polarize the system. Mo and Ti NPs showed the peak positions at 6.0 eV for NPs of size close to 75 nm. Gold NPs exhibit the lowest peak energy of 2.5 eV for a size range 10 to 250 nm, which decreases slightly with increasing NPs size, while Rh, Mo, and Ag NPs exhibit the highest peak energies for small NPs. Rh, Re, Zn, Mo, Ti, and Ta have peak energies above 3.5 eV for NPs below 150 nm. There is convergence of the LSPR peak position for NPs of 275 to 400 nm, and all transition metal NPs showed the same peak energies, which were decreasing linearly for the same NPs size.

3.2. Size-dependence of LSPR peak FWHM

The dependence of FWHM of the LSPR extinction peak on NP size for the investigated metals is shown in Fig. 3. The FWHM provided a direct measure of plasmon damping, incorporating both radiative and non-radiative loss mechanisms.

For all metals, the FWHM initially increased with NP size, reaching a broad maximum in the intermediate size range (~ 150…250 nm), where competition between absorption and scattering losses is the strongest. At larger sizes, the FWHM decreases due to reduced coherence of electron oscillations and the dominance of radiative damping [22, 23]. The particle sizes, where the maximum spectral broadening occurs, are marked by the dashed lines (Fig. 3). This broadening is associated with the onset of strong radiative damping and multipolar plasmon excitation. Differences in FWHM magnitude and trend reflect material-dependent intrinsic losses and size-dependent damping mechanisms.

Among the UTMs, Ta exhibited the smallest line-width across most sizes, while Ti and Mo displayed the strongest damping, particularly at intermediate sizes. Zn, Rh, Re, and Sc exhibited comparatively moderate linewidths, with values approaching those of noble metals within specific size and energy regimes. These results demonstrate that, despite stronger intrinsic damping, several UTMs can support relatively well-defined plasmonic resonances under appropriate size conditions.

Ta exhibits the smallest FWHM for all NP sizes, while Ti showed the maximum FWHM values specifically between 150 and 225 nm. At 3.0 eV, Zn presented broadening less than 1.0 eV for peak energies above 5.0 eV, which is comparable with the FWHM exhibited by silver and gold below 2.0 eV. FWHM for Mo and Ta NPs showed more pronounced broadening for smaller NPs.

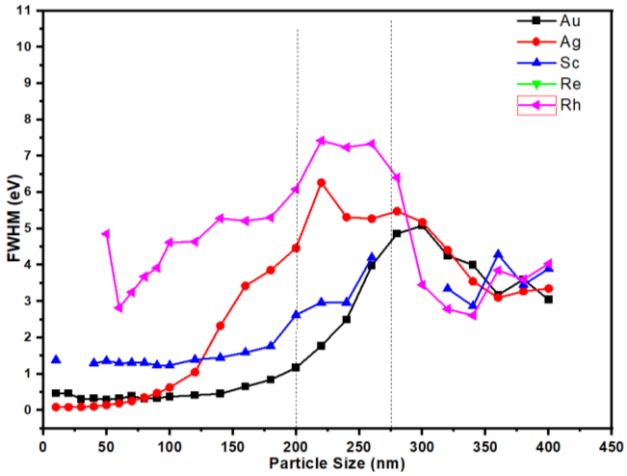

(a)

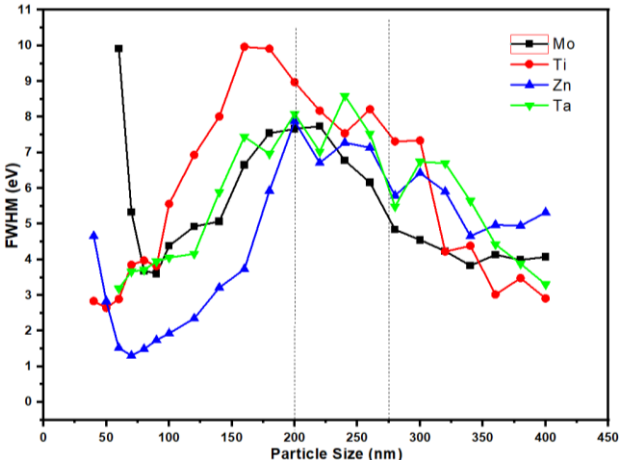

(b)

Fig. 3. Variation of FWHM of the LSPR as a function of NP size for selected metallic NPs. (a) Au, Ag, Sc, Re, and Rh; (b) Mo, Ti, Zn, and Ta. The dashed vertical lines indicate the intermediate particle sizes, where the maximum spectral broadening occurs.

Mo attains maximum energy at 7.5 eV for an NP size of 200 nm, while Ta attains maximum energy for an NP size of 50 nm. Zn, Rh, Re, and Sc NPs exhibited relatively narrower FWHM compared to Mo and Ta, potentially due to lower electron density and scattering rates. This is because interband transitions and surface scattering are more dominant in this range, which broadens the plasmon band [24, 25]. The peak sharpness decreased for NPs of Au, Sc, Ag, and Zn in the size range of 10 to 200 nm. Below approximately 50 nm, Mo, Ta, Ti, Rh, Re, and Zn do not have significant peaks. Between 200 and 275 nm, each transition metal NPs displayed maximum broadening at different energies, with Rh having the most broadened peak at 9.5 eV, while Au had the least broadened peak at 3.5 eV. Apart from Au and Sc, which exhibited narrowing of the FWHM from 275 nm, the rest of the metals exhibited narrowing of the FWHM from 200 nm and beyond. Mo NPs at 200 nm show the bimodal LSPR peak.

4. Conclusion

This study has systematically investigated the size-dependent localized surface plasmon resonance and damping behavior of selected unconventional transition metal NPs using full Mie theory. By analyzing NP sizes from 10 to 400 nm, the work demonstrated that UTMs can exhibit tunable LSPR responses across a broad spectral range, including the ultraviolet region, where noble metals are limited by interband transitions. While Au and Ag remain superior in terms of narrow linewidths and low damping, several UTMs displayed plasmonic characteristics comparable to noble metals within specific size regimes. The convergence of LSPR energies at large particle sizes underscores the dominant role of retardation and dynamic depolarization effects. These findings highlighted the potential of UTMs as alternative plasmonic materials for broadband optical, catalytic, and energy-related applications. Future work may explore shape effects, alloying, and surface functionalization to further optimize their plasmonic performance.

References

1. Zhao J., Xue S., Ji R. *et al*. Localized surface plasmon resonance for enhanced electrocatalysis. *Chem. Soc. Rev*. 2021. **50**, No 21. P. 12070–12097. https://doi.org/10.1039/d1cs00237f.
2. Khurana K., Jaggi N. Localized surface plasmonic properties of Au and Ag nanoparticles for sensors: a review. *Plasmonics*. 2021. **16**, No 4. P. 981–999. https://doi.org/10.1007/s11468-021-01381-1.
3. Todorov R., Hristova-Vasileva T. Review of the current state of optical characterization and design of electronic states in plasmonic materials – From noble metals to silverene and goldene. *Nanomaterials*. 2025. **15**, No 20. P. 1548. https://doi.org/10.3390/nano15201548.
4. Demydov P.V., Lopatynskyi A.M., Hudzenko I.I., Chegel V.I. The approaches for localized surface plasmon resonance wavelength position tuning. Short review. *SPQEO*. 2021. **24**. P. 304–311. https://doi.org/10.15407/spqeo24.03.304.
5. Kim S., Kim J.-M., Park J.-E., Nam J.-M. Nonnoble-metal-based plasmonic nanomaterials: recent advances and future perspectives. *Adv. Mater*. 2018. **30**, No 42. P. 1704528. https://doi.org/10.1002/adma.201704528.
6. Hartland G.V., Optical studies of dynamics in noble metal nanostructures. *Chem. Rev*. 2011. **111**, No 6. P. 3858–3887. https://doi.org/10.1021/cr1002547.
7. Bhattacharya C., Saji S.E., Mohan A. *et al.* Sustainable nanoplasmon-enhanced photoredox reactions: Synthesis, characterization, and applications. *Adv. Energy Mater*. 2020. **10**, No 40. P. 2002402. https://doi.org/10.1002/aenm.202002402.
8. Cortés E., Wendisch F.J., Sortino L. *et al*. Optical metasurfaces for energy conversion. *Chem. Rev*. 2022. **122**, No 19. P. 15082–15176. https://doi.org/10.1021/acs.chemrev.2c00078.

9. Sayed M., Yu J., Liu G., Jaroniec M. Non-noble plasmonic metal-based photocatalysts. *Chem. Rev*. 2022. **122**, No 11. P. 10484–10537. https://doi.org/10.1021/acs.chemrev.1c00473.
10. Hopper E.R., Boukouvala C., Asselin J. *et al*. Opportunities and challenges for alternative nanoplasmonic metals: Magnesium and beyond. *J. Phys. Chem. C*. 2022. **126**, No 26. P. 10630–10643. https://doi.org/10.1021/acs.jpcc.2c01944.
11. Shi, H., Zhu X., Zhang S. *et al*. Plasmonic metal nanostructures with extremely small features: New effects, fabrication and applications. *Nanoscale Adv*. 2021. **3**, No 15. P. 4349–4369. https://doi.org/10.1039/d1na00237f.
12. Zhou, H., Li D., Lv Q. *et al*. Integrative plasmonics: Optical multi-effects and acousto-electric-thermal fusion for biosensing, energy conversion, and photonic circuits. *Chem. Soc. Rev*. 2025. **54**. P. 5342–5432. https://doi.org/10.1039/d4cs00427b.
13. Thapa D.K., Biswas S. Plasmonics for chemical transformation: From fundamentals to the cutting-edge applications. *ChemPhysChem*. 2025. **26**, No 19. P. e202401102. https://doi.org/10.1002/cphc.202401102.
14. Cortie M.B., Arnold M.D., Keast V.J. The quest for zero loss: Unconventional materials for plasmonics. *Adv. Mater*. 2020. **32**, No 18. P. 1904532. https://doi.org/10.1002/adma.201904532.
15. Farooq S., Zezell D.M. Advances in metallic-based localized surface plasmon sensors for enhanced tropical disease detection: a comprehensive review. *Plasmonics*. 2024. **19**, No 4. P. 1721–1742. https://doi.org/10.1007/s11468-023-02109-z.
16. Wang P., Nasir M.E., Krasavin A.V. *et al*. Plasmonic metamaterials for nanochemistry and sensing. *Acc. Chem. Res*. 2019. **52**, No 11. P. 3018–3028. https://doi.org/10.1021/acs.accounts.9b00325.
17. Marhaba S. Effect of size, shape and environment on the optical response of metallic nanoparticles. Vol. 1. In: *Noble and Precious Metals – Properties, Nanoscale Effects and Applications*, Seehra M.S., Bristow A.D. (Eds). IntechOpen, 2018. https://doi.org/10.5772/intechopen.71574.
18. Johnson P.B., Christy R.-W. Optical constants of the noble metals. *Phys. Rev. B.* 1972. **6**, No 12. P. 4370. https://doi.org/10.1103/physrevb.6.4370.
19. Masheli M.H., Eyvazi S., Aghdaee M., Amjad J.M. LSPR of nanoparticles inside strong absorbent medium. *J. Phys. Chem. C*. 2023. **127**, No 49. P. 23696–23705. https://doi.org/10.1021/acs.jpcc.3c04682.
20. Grainger R.G., Lucas J., Thomas G.E., Ewen G.B.L. Calculation of Mie derivatives. *Appl. Opt*. 2004. **43**. P. 5386–5393. https://doi.org/10.1364/ao.43.005386.
21. Akimov Y.A. Mie scattering theory: A review of physical features and limitations. arXiv preprint arXiv:2401.04146v1 [physics.optics] 08 Jan 2024.
22. Xie P., Li D., Chen Y. *et al*. Enhanced coherent interaction between monolayer WS 2 and film-coupled nanocube open cavity with suppressed incoherent damping pathway. *Phys. Rev. B*. 2020. **102**, No 11. P. 115430. https://doi.org/10.1103/physrevb.102.115430.
23. Devkota T., Brown B.S., Beane G. *et al*. Making waves: Radiation damping in metallic nanostructures. *J. Phys. Chem. C*. 2019. **151**, No 8. https://doi.org/10.1063/1.5117230.
24. Kolwas K., Derkachova A. Impact of the interband transitions in gold and silver on the dynamics of propagating and localized surface plasmons. *Nanomaterials*. 2020. **10**, No 7. P. 1411. https://doi.org/10.3390/nano10071411.
25. Fonseca Guzman M.V., Ross M.B. Radiative contributions dominate plasmon broadening for post-transition metals in the ultraviolet. *J. Phys. Chem. C*. 2021. **125**, No 35. P. 19428–19437. https://doi.org/10.1021/acs.jpcc.1c03895.

Authors and CV

Faith Sila, junior researcher at the Department of Physical Sciences, South Eastern Kenya University. She is the current assistant editor in the Physics Society of Kenya and a lecturer at the Umma University. The area of her scientific interests includes Physics Education, Geophysics, nanoplasmonics. https://orcid.org/0009-0003-0808-5088

Benjamin Mbaluka John, defended his PhD thesis in Physics (Material Physics) in 2022 at the Jomo Kenyatta University of Agriculture and Technology. He works at the Bomet University. Authored 7 publications. The area of his scientific interests include physics and nanotechnology, semiconductor materials, hetero and hybrid structures and devices (solar cells), high voltage power systems, electronics, as well as the modeling and the application of artificial intelligence-based models for new material discovery and the analysis of power systems.
E-mail: bmbaluka@buc.ac.ke

Martin Riara, defended his PhD thesis in Materials Science and Engineering in 2019 at the Wuhan University of Technology. He is a Senior Lecturer at the Tharaka University. His scientific interests include plasmonic behavior of transition metals, physics and technology of polymeric materials, radiation safety of construction materials, and healing mechanisms of asphaltic materials. Other areas of interest include modeling and analysis of the extracellular electrical potential in plants under different stimuli.
E-mail: riaramartin@gmail.com,
http://orcid.org/0000-0002-9964-8848

Ngei Katumo earned his PhD in Electrical Engineering from the Karlsruhe Institute of Technology. His doctoral research centered on persistent phosphors and their innovative applications in anti-counterfeiting and thermometric sensing using smartphones. Dr.-Ing. Ngei Katumo has authored more than 15 scientific publications, and his research interests include material spectroscopy, renewable energy, and smart sensing technologies.
https://orcid.org/0000-0002-1106-4996

Authors' contributions

Sila F.: conceptualization, simulation, analysis, writing – original draft preparation, writing – review & editing.
Mbaluka B.: conceptualization, supervision, simulation, analysis, writing – original draft preparation, review & editing.
Riara M.: supervision, data curation, writing – review & editing, project administration.
Ngei P.: data curation, analysis, writing – review & editing.

Локалізований поверхневий плазмонний резонанс та механізми демпфування у перехідних металах

F. Sila, B. Mbaluka, M. Riara & N. Katumo

Анотація. У цій роботі представлено розраховану залежність параметрів локалізованого поверхневого плазмонного резонансу (LSPR) та механізму затухання від розміру наночастинок (НЧ) нетрадиційних перехідних металів, зокрема, цинк, срібло, родій, реній, молібден, тантал, титан та скандій, розмірами від 10 до 400 нм. У дослідженні було використано теорію Мі для визначення енергії піків, амплітуди та півширини (FWHM) LSPR як функції розміру, форми та типу матеріалу. Ми виявили, що параметри LSPR залежать від електронної структури та механізмів затухання. Амплітуда LSPR систематично зменшувалася для окремих НЧ розмірами 10…200 нм, після чого спостерігалася аналогічна тенденція через випромінювальне затухання. Au, Sc та Ag – єдині металеві НЧ, які демонстрували значну півширину приблизно нижчу ніж 40 нм. Для всіх досліджених НЧ перехідних металів, менші НЧ демонстрували вище поглинання та менше розсіювання, тоді як більші НЧ демонстрували вужчу півширину та зміщені в червону область піки LSPR через ефекти затримки та багатополярне плазмонне збудження. Аналіз показує, що деякі НЧ перехідних металів демонструють оптичні характеристики, подібні до характеристик золота, срібла та міді, що робить їх гарною альтернативою до вказаних при певних розмірах наночастинок.

Ключові слова: нетрадиційні перехідні метали, розсіювання, поглинання, локалізований поверхневий плазмонний резонанс, затухання, благородні метали.